

QUT Digital Repository:
<http://eprints.qut.edu.au/>



Hibiki, Takashi and Situ, Rong and Mi, Ye and Ishii, Mamoru (2003) Formulation of one-dimensional interfacial area transport equation in subcooled boiling flow. In Chang, Soon Heung and Baek, Won-Pil and Rempe, Joy, Eds. *Proceedings 10th International Topical Meeting on Nuclear Reactor Thermal Hydraulics (NURETH-10)*(A00401), Seoul, Korea.

© Copyright 2003 (please consult author)

FORMULATION OF ONE-DIMENSIONAL INTERFACIAL AREA TRANSPORT EQUATION IN SUBCOOLED BOILING FLOW

Takashi HIBIKI

Research Reactor Institute, Kyoto University
Kumatori, Sennan, Osaka 590-0494, Japan
E-mail address hibiki@rri.kyoto-u.ac.jp

Rong Situ, Ye Mi, Mamoru ISHII

School of Nuclear Engineering, Purdue University
400 Central Drive, West Lafayette, IN 47907-2017, USA
E-mail address ishii@ecn.purdue.edu

KEY WORDS

Interfacial area transport, Subcooled boiling flow, Bubble layer thickness

ABSTRACT

In relation to the formulation of one-dimensional interfacial area transport equation in a subcooled boiling flow, the bubble-layer thickness model was introduced to avoid many covariances in cross-sectional averaged interfacial area transport equation in the subcooled boiling flow. The one-dimensional interfacial area transport equation in the subcooled boiling flow was formulated by partitioning a flow region into two regions; boiling two-phase (bubble-layer) region and liquid single-phase region. The bubble-layer thickness model assuming the square void peak in the bubble-layer region was developed to predict the bubble-layer thickness of the subcooled boiling flow. The obtained model was evaluated by void fraction profile measured in an internally heated annulus. It was shown that the bubble-layer thickness model could be applied to predict the bubble-layer thickness as well as the void fraction profile. In addition, the constitutive equation for the distribution parameter of the boiling flow in the internally heated annulus, which was used for formulating the bubble-layer thickness model, was developed based on the measured data. The model developed in this study will eventually be used for the development of reliable constitutive relations, which reflect the true transfer mechanisms in subcooled boiling flows.

1. INTRODUCTION

In 1996, the workshop on transient thermal-hydraulic and neutronic code requirements was held to discuss (1) current and prospective plans of thermal hydraulic codes development; (2) current and

anticipated uses of thermal-hydraulic codes; (3) advances in modeling of thermal-hydraulic phenomena and associated additional experimental needs; (4) numerical methods in multi-phase flows; and (5) programming language, code architectures and user interfaces [Ebert, 1997]. The workshop consensus identified some important action items to be addressed by the international community in order to maintain and improve the calculation capability. One of the important action items is the introduction of the interfacial area transport equation to the interfacial transfer terms in the two-fluid model.

The interfacial area transport equation can be obtained by considering the fluid particle number density transport equation analogous to Boltzmann's transport equation [Ishii & Kojasoy, 1993; Kocamustafaogullari & Ishii, 1995]. It can replace the traditional flow regime maps and regime transition criteria that do not dynamically represent the changes in interfacial structure [Ishii, 1996; Uhle et al., 1996]. The changes in the two-phase flow structure are predicted mechanistically by introducing the interfacial area transport equation. The effects of the boundary conditions and flow development are efficiently modeled by this transport equation. Such a capability does not exist in the current thermal-hydraulic system analysis codes [Uhle et al., 1996]. Thus, a successful development of the interfacial area transport equation can make a quantum improvement in the two-fluid model formulation.

For this purpose, continuous efforts, which were extensively surveyed in the previous paper [Hibiki & Ishii, 2000b; Hibiki & Ishii, 2002], have been made analytically and experimentally. In the first stage of the development of the interfacial area transport equation, one-dimensional adiabatic flow was the focus. In the adiabatic flow, sink and source terms of the interfacial area concentration due to phase change can be dropped in the interfacial area transport equation. The one-dimensional form of the interfacial area transport equation can be obtained by applying cross-sectional area averaging over three-dimensional form of the interfacial area transport equation. However, the exact mathematical expressions for the area-averaged sink and source terms would involve many covariances that might further complicate the one-dimensional problem. However, since these local terms are originally obtained from a finite volume element of the mixture [Hibiki & Ishii, 2000a; Wu et al., 1998], the functional dependence of the area-averaged source and sink terms on the averaged parameters could be assumed to be approximately the same if the hydraulic diameter of the flow path was considered as the length scale of the finite element [Wu et al., 1998]. Therefore, it has been assumed that three-dimensional sink and source terms with the parameters averaged within the cross-sectional area are still applicable for the area-averaged sink and source terms in the one-dimensional form of the interfacial area transport equation [Wu et al., 1998]. This assumption would be valid for relatively uniform local flow parameters over a flow channel like those in an adiabatic vertical flow. Under this assumption, the interfacial area transport equation for the one-dimensional adiabatic flow was developed successfully by modeling sink and source terms of the interfacial area concentration due to bubble coalescence and breakup [Hibiki & Ishii, 2000a; 2000b; 2002; Hibiki et al., 2001; Wu et

al., 1998]. In the next stage, subcooled boiling flow would be the focus, and a preliminary local measurement for interfacial area concentration was initiated for subcooled boiling water flow in an internally heated annulus [Bartel et al.; 2001]. To develop the interfacial area transport equation for subcooled boiling flows, sink and source terms due to phase change should be modeled based on rigorous and extensive boiling flow data. In addition, since phase distribution pattern in subcooled boiling flow would not be uniform over a flow channel, the one-dimensional form of the interfacial area transport equation should be reformulated by taking account of the non-uniformity in the phase distribution pattern. The subcooled boiling flow may be characterized as two distinctive flow regions, namely (1) boiling two-phase (bubble layer) region where the void fraction profile may approximately be assumed to be uniform, and (2) liquid single-phase region where the void fraction may be assumed to be zero. Many covariances due to applying cross-sectional area averaging over three-dimensional form of the interfacial area transport equation would be avoided by taking the average over the bubble layer.

From this point of view, this study aims at developing the bubble-layer thickness model to reformulate the one-dimensional interfacial area transport equation in subcooled boiling flow. The developed bubble-layer thickness model is evaluated by local void fraction data in subcooled boiling flow, which were taken by using an internally heated annulus consisting of an inner heater rod with a diameter of 19.1 mm and an outer round tube with an inner diameter of 38.1 mm [Bartel et al., 2001; Ishii et al., 1999b; 2000]. The model developed in this study will eventually be used for the development of reliable constitutive relations, which reflect the true transfer mechanisms in subcooled boiling flows.

2. FORMULATION OF ONE-GROUP INTERFACIAL AREA TRANSPORT EQUATION FOR SUBCOOLED BOILING FLOW

For the purpose of modeling interfacial area transport, Ishii and Kocamustafaogullari [1993; 1995] obtained the interfacial area transport equation based on statistical mechanics. The fluid particle number density distribution changes with the fluid particle contraction and expansion, entering and leaving, coalescence and disintegration, evaporation and condensation, nucleation and collapse. Simply accounting for these effects in a control volume yields the fluid particle transport equation:

$$\frac{\partial f}{\partial t} + \nabla \cdot (f \vec{v}_p) + \frac{\partial}{\partial V} \left(f \frac{dV}{dt} \right) = \sum_j S_j + S_{ph}, \quad (1)$$

where $f(\vec{x}, V, t)$ is the particle density distribution function, which is assumed to be continuous and specifies the probable number density of fluid particles at a given time t , in the spatial range $d\vec{x}$

about a position \vec{x} , with particle volumes between V and $V+dV$. $\vec{v}_p(\vec{x}, V, t)$ denotes the particle velocity of volumes between V and $V+dV$ at a given time t in the spatial range $d\vec{x}$ about a position \vec{x} . For small bubbles, the internal circulation can be neglected. Accordingly, the particle velocity, \vec{v}_p , is identical to the gas-phase velocity, \vec{v}_g [Wu et al., 1998]. The interaction term, $\sum_j S_j$, represents the net rate of change in the particle density distribution due to the particle coalescence and breakup processes. The second term of the right hand side, S_{ph} , is the fluid particle source or sink rate due to the phase change. For example, for a one-component bubbly flow, S_{ph} represents the bulk liquid bubble nucleation rate due to homogeneous and heterogeneous nucleation, and the collapse rate due to condensation for the subcooled boiling flow. The wall nucleation rate which is not included in S_{ph} must be specified as a boundary condition. The third term of the left-hand side in Eq.(1) represents the rate of change in the particle density distribution due to the pressure change and/or phase changes appearing on existing interfaces.

The interfacial area concentration transport equation of fluid particles can be obtained by multiplying the particle number density transport equation by the average interfacial area, $A_i(V)$, which is independent of the spatial coordinate system. This yields the following equation [Ishii et al., 1999a; Shraiber, 1996]:

$$\frac{\partial f A_i(V)}{\partial t} + \nabla \cdot \{f \vec{v}_g A_i(V)\} + A_i(V) \frac{\partial}{\partial V} \left(f \frac{dV}{dt} \right) = \sum_j S_j A_i(V) + S_{ph} A_i(V). \quad (2)$$

For practical purposes, the fluid particle interfacial area transport equation is too detailed. Hence, it would be much more useful to average an interfacial area transport equation over particle size groups that are determined according to particle mobilities. As a general approach, two-group interfacial area transport equations have recently been proposed by treating the bubbles in two groups such as the spherical/distorted bubble group (group one) and the cap/slug bubble group (group two) [Uhle et al., 1998]. If only one-group bubbles are considered, the interfacial area transport equation can easily be obtained by integrating Eq. (2) from V_{min} to V_{max} and applying the Leibnitz rule. Then, we have the three-dimensional interfacial transport equation [Ishii et al., 1999a]:

$$\frac{\partial a_i}{\partial t} + \nabla \cdot (a_i \vec{v}_g) = \frac{2}{3} \frac{a_i}{\alpha} \left(\frac{\partial \alpha}{\partial t} + \nabla \cdot \alpha \vec{v}_g \right) + \frac{1}{3\psi} \left(\frac{\alpha}{a_i} \right)^2 \sum_j R_j + \pi D_{bc}^2 \left\{ 1 - \frac{2}{3} \left(\frac{D_{bc}}{D_{Sm}} \right) \right\} R_{ph}. \quad (3)$$

where R_j and R_{ph} are the rate of change of particle number due to coalescence or breakup, and phase change, respectively. ψ is the shape factor and defined by

$$\psi = \frac{1}{36\pi} \left(\frac{D_{Sm}}{D_e} \right)^3, \quad (4)$$

where D_e is the volume equivalent diameter, and therefore, $\psi=1/36\pi$ for a spherical bubble. D_{bc} is the critical bubble size beyond which it is possible for bubbles to grow due to evaporation, or for clusters of molecules to serve as nuclei for bubbles. For a static case, D_{bc} is given by

$$D_{bc} = \frac{4\sigma T_{sat}}{\rho_g \Delta i_{fg} (T_f - T_{sat})}. \quad (5)$$

where σ , T_{sat} , ρ_g , Δi_{fg} , and T_f are the surface tension, the saturation temperature, the gas density, the latent heat, and the liquid temperature, respectively.

The simplest form of the one-group interfacial area transport equation is the one-dimensional formulation obtained by applying cross-sectional area averaging over Eq. (3). However, the exact mathematical expressions for the area-averaged source and sink terms would involve many covariances that might further complicate the one-dimensional problem. For an adiabatic vertical flow, phase distribution pattern can be considered to be relatively uniform, and therefore the covariances can be neglected [Wu et al., 1998]. Thus, three-dimensional sink and source terms with the parameters averaged within the cross-sectional area are still applicable for the area-averaged sink and source terms in the one-dimensional form of the interfacial area transport equation. However, for subcooled boiling flow, phase distribution pattern may not be assumed to be uniform, resulting in many covariances in the one-dimensional interfacial area transport equation. To avoid the covariances, the following simple model is introduced to formulate one-dimensional interfacial area transport equation for subcooled boiling flow. For subcooled boiling flow, the bubbles mainly exist near a heated wall, whereas almost no bubble exists far from the heated wall. Therefore, the flow path may be divided into two regions, namely (i) boiling two-phase (bubble layer) region where the void fraction profile can be assumed to be uniform, and (ii) liquid single-phase region where the void fraction can be assumed to be zero. Thus, the one-group interfacial area transport equation averaged over the bubble-layer region is obtained as:

$$\begin{aligned} \frac{\partial \langle a_i \rangle_B}{\partial t} + \frac{d}{dz} \left(\langle a_i \rangle_B \langle \langle v_{gz} \rangle \rangle_B \right) &= \left(\frac{2 \langle a_i \rangle_B}{3 \langle \alpha \rangle_B} \right) \left(\frac{\partial \langle \alpha \rangle_B}{\partial t} + \frac{d}{dz} \left\{ \langle \alpha \rangle_B \langle \langle v_{gz} \rangle \rangle_B \right\} \right) \\ + \frac{1}{3\psi} \left(\frac{\langle \alpha \rangle_B}{\langle a_i \rangle_B} \right)^2 \sum_j \langle R_j \rangle_B + \pi D_{bc}^2 \left\{ 1 - \frac{2}{3} \left(\frac{D_{bc}}{D_{Sm}} \right) \right\} \langle R_{ph} \rangle_B + \langle \phi_w \rangle_B \end{aligned} \quad (6)$$

where $\langle \rangle_B$ means the quantity averaged over the bubble-layer region, and ϕ_w is the wall nucleation source, which is the most important term for subcooled boiling flow. The cross-sectional area averaged quantities can be given by the product of the quantity averaged over the bubble-layer region and A_B/A_C , where A_B and A_C are the area of the bubble-layer region and the cross-sectional area, respectively.

It should be noted here that three-dimensional source and sink terms with the parameters averaged within the bubble-layer region would be still applicable for the source and sink terms averaged within

the bubble-layer region in Eq.(6) on the following ground. Since these local terms in three-dimensional interfacial area transport equation are originally obtained from a finite volume element of the mixture, the functional dependence of the source and sink terms averaged over the bubble-layer region on the parameters averaged over the bubble-layer region should be approximately the same if the bubble-layer thickness is considered as the length scale of the finite element.

3. DEVELOPMENT OF BUBBLE-LAYER THICKNESS MODEL

As explained in the previous section, it is anticipated that a void peaking near a heated wall would appear in subcooled boiling flow. In the subcooled boiling flow, relatively uniform phase distribution over a flow channel may not be assumed, resulting in many covariances in one-dimensional interfacial area transport equation. To avoid the covariances, the bubble-layer model shown in Fig.1 is introduced to formulate one-dimensional interfacial area transport equation. Here, an internally heated annulus is taken as an example. In this model, a flow path is divided into two regions, namely (i) boiling two-phase (bubble layer) region where the void fraction profile is assumed to be uniform, and (ii) liquid single-phase region where the void fraction is assumed to be zero. In Fig.1, α , x , R_0 , α_{WP} , x_{WP} , and R are the local void fraction, the radial coordinate measured from the center of the heater rod, the radius of the heater rod, the void fraction at the assumed square void peak, the bubble-layer thickness, and the radius of the outer round tube, respectively. In what follows, the bubble-layer thickness in an internally heated annulus will be derived.

The profile of mixture volumetric flux, j , in the flow channel is approximated as:

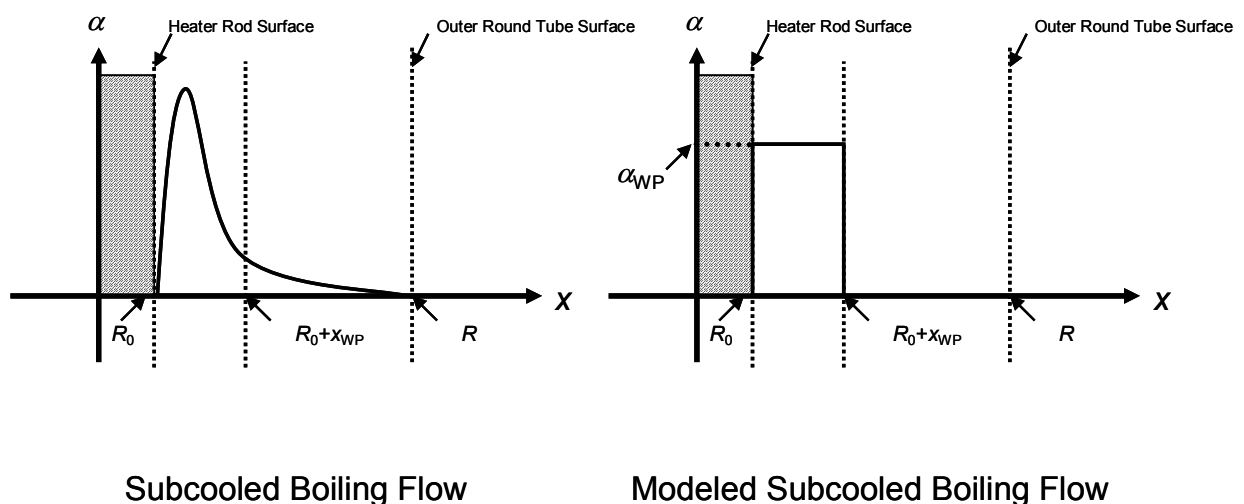


Fig.1. Schematic diagram of modeled subcooled boiling flow in bubble-layer thickness model for an internally heated annulus.

$$j = \frac{n+1}{n} \langle j \rangle \left\{ 1 - \left| 1 - \frac{2r}{R-R_0} \right|^n \right\}, \quad (7)$$

where n and r are the exponent and the radial coordinate measured from the heater rod surface, respectively, and $\langle \rangle$ means the cross-sectional averaged quantity. As shown in Fig.1, for the purpose of the bubble-layer model, the profile of the void fraction is assumed to be square peak near the wall (bubble-layer region), and is approximated as:

$$\begin{aligned} \alpha &= \alpha_{WP} \quad \text{for } 0 \leq r \leq x_{WP} \\ \alpha &= 0 \quad \text{for } x_{WP} \leq r \leq R - R_0 \end{aligned} \quad (8)$$

The distribution parameter, C_0 , can be obtained by mixture volumetric flux and void fraction profiles as [Zuber & Findlay, 1965]:

$$C_0 = \frac{\langle \alpha j \rangle}{\langle \alpha \rangle \langle j \rangle}. \quad (9)$$

From Eqs.(7)-(9), one can obtain the distribution parameter for subcooled boiling flow analytically as:

$$C_0 = \frac{n+1}{2n} \frac{R^2 - R_0^2}{x_{WP}(x_{WP} + 2R_0)} \times \left[\frac{2R_0}{R+R_0} \frac{2x_{WP}}{R-R_0} + \frac{R-R_0}{2(R+R_0)} \left(\frac{2x_{WP}}{R-R_0} \right)^2 + \frac{1}{n+1} \left\{ \left(1 - \frac{2x_{WP}}{R-R_0} \right)^{n+1} - 1 \right\} - \frac{R-R_0}{R+R_0} \frac{1}{n+2} \left\{ \left(1 - \frac{2x_{WP}}{R-R_0} \right)^{n+2} - 1 \right\} \right]$$

$$\text{for } 0 \leq x_{WP} \leq \frac{R-R_0}{2},$$

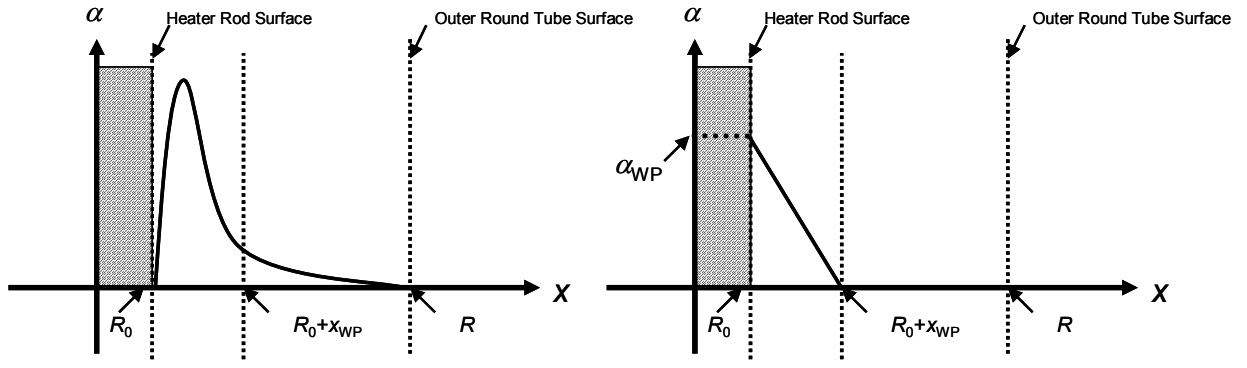
$$\begin{aligned} C_0 &= \frac{n+1}{2n} \frac{R^2 - R_0^2}{x_{WP}(x_{WP} + 2R_0)} \times \left\{ \frac{n(3n+5)R_0 + n(n+3)R}{2(n+1)(n+2)(R+R_0)} \right. \\ &+ \left. \left(\frac{2x_{WP}}{R-R_0} - 1 \right) + \frac{R-R_0}{2(R+R_0)} \left(\frac{2x_{WP}}{R-R_0} - 1 \right)^2 - \frac{1}{n+1} \left(\frac{2x_{WP}}{R-R_0} - 1 \right)^{n+1} - \frac{R-R_0}{R+R_0} \frac{1}{n+2} \left(\frac{2x_{WP}}{R-R_0} - 1 \right)^{n+2} \right\} \\ \text{for } \frac{R-R_0}{2} &\leq x_{WP} \leq R - R_0. \end{aligned} \quad (10)$$

The area-averaged void fraction can be obtained as:

$$\langle \alpha \rangle = \frac{2\alpha_{WP}x_{WP}}{R^2 - R_0^2} \left(R_0 + \frac{x_{WP}}{2} \right). \quad (11)$$

As can be seen in Eq.(10), one can estimate the bubble-layer thickness provided that the distribution parameter and the exponent, n , are given.

As shown in Fig.2, for the purpose of better estimation in void fraction profile, the profile of void fraction may be assumed to be right triangle peak near the wall, and is approximated as:



Subcooled Boiling Flow

Modeled Subcooled Boiling Flow

Fig.2. Schematic diagram of modeled subcooled boiling flow in void profile model for an internally heated annulus.

$$\alpha = -\frac{\alpha_{WP}}{x_{WP}}(r-x_{WP}) \text{ for } 0 \leq r \leq x_{WP} \quad (12)$$

$$\alpha = 0 \text{ for } x_{WP} \leq r \leq R - R_0$$

From Eqs.(7), (9) and (12), one can obtain the distribution parameter for subcooled boiling flow analytically as:

$$C_0 = \frac{n+1}{n} \frac{(R-R_0)^2}{x_{WP}^2 \left(\frac{4}{3}x_{WP} + 4R_0 \right)} \times \left[\left(1 - \frac{2x_{WP}}{R-R_0} \right)^2 \left[\frac{1}{3}(R+2R_0+x_{WP}) - \left(1 - \frac{2x_{WP}}{R-R_0} \right)^n \frac{2\{R+(n+2)R_0+(n+1)x_{WP}\}}{(n+1)(n+2)(n+3)} \right] - \left\{ \frac{R+2R_0+3x_{WP}}{3} - \frac{2(R+R_0)x_{WP}}{R-R_0} - \frac{R+R_0}{n+1} \left(1 - \frac{2x_{WP}}{R-R_0} \right) + \frac{2}{n+2}(R-x_{WP}) - \frac{1}{n+3}(R-R_0) \right\} \right]$$

$$\text{for } 0 \leq x_{WP} \leq \frac{R-R_0}{2},$$

$$C_0 = \frac{n+1}{n} \frac{(R-R_0)^2}{x_{WP}^2 \left(\frac{4}{3}x_{WP} + 4R_0 \right)} \times \left[\left(1 - \frac{2x_{WP}}{R-R_0} \right)^2 \left[\frac{1}{3}(R+2R_0+x_{WP}) - \left(\frac{2x_{WP}}{R-R_0} - 1 \right)^n \frac{2\{R+(n+2)R_0+(n+1)x_{WP}\}}{(n+1)(n+2)(n+3)} \right] - \left\{ \frac{R+2R_0+3x_{WP}}{3} - \frac{2(R+R_0)x_{WP}}{R-R_0} - \frac{R+R_0}{n+1} \left(1 - \frac{2x_{WP}}{R-R_0} \right) + \frac{2}{n+2}(R-x_{WP}) - \frac{1}{n+3}(R-R_0) \right\} \right]$$

$$\text{for } \frac{R - R_0}{2} \leq x_{WP} \leq R - R_0, \quad (13)$$

The area-averaged void fraction can be obtained as:

$$\langle \alpha \rangle = \frac{\alpha_{WP} x_{WP}}{R^2 - R_0^2} \left(R_0 + \frac{x_{WP}}{3} \right). \quad (14)$$

4. RESULTS AND DISCUSSION

4.1. Data base used for evaluation of bubble-layer model

In order to evaluate the derived bubbly-layer thickness model, Eq.(10), and void profile model, Eq.(13), the authors measured local flow parameters of subcooled water boiling flows in an internally heated annulus at the Thermal-hydraulics and Reactor Safety Laboratory in Purdue University [Bartel et al., 2001; Ishii et al., 1999b; 2000]. An experimental facility used in the experiment is scaled to a prototypic BWR based on scaling criteria for geometric, hydrodynamic, and thermal similarities [Bartel et al., 2001]. The test section is an annular geometry that is formed by a clear polycarbonate tube on the outside and a cartridge heater on the inside. The inner diameter of the outer tube is 38.1 mm. The overall length of the heater is 2670 mm and has a 19.1 mm outer diameter. The heated section of the heater rod is 1730 mm long. The maximum power of the heater is 20 kW and has a maximum surface heat flux of 0.193 MW/m². Local measurements of void fraction, interfacial area concentration, and interfacial velocity were performed by using the double-sensor conductivity probe method. The double-sensor conductivity probe was held and positioned along the radial direction using a traversing mechanism. Data were taken at four different axial locations as well as eight radial positions. Flow conditions in the experiments are listed in Table 1. The details of the experimental loop and experimental procedure are found in the previous paper [Bartel et al., 2001] and reports [Ishii et al., 1999b; 2000].

4.2. Development of constitutive equation for distribution parameter of subcooled boiling flow in an internally heated annulus

The bubble-layer thickness can be obtained provided the distribution parameter and the exponent, n , are given. Ishii [Ishii, 1974] developed the distribution parameter in developing flow due to boiling based on the following extensive discussion. For a flow with generation of void at the wall due to nucleation, the distribution parameter should have a near-zero value at the beginning of the two-phase flow region. With the increase in the cross-sectional mean void fraction, the peak of the local void fraction moves from the near-wall region to the central region. This will lead to the

Table 1. Experimental conditions of the database.

References	Run No.	G [kg/m ² s]	q'' [MW/m ²]	ΔT_{sub} [K]	z_H/D_H [-]	$\langle \alpha \rangle$ [-]	C_0 [-]
Bartel et al. (2001) Ishii et al. (1999b)	R1-4-1	470	0.105	8.9	99.1	0.0165	0.8972
	R2-4-2	922	0.147	3.6	93.8	0.0290	0.9619
	R3-4-1	701	0.128	6.1	99.1	0.0203	0.9209
	R4-4-1	701	0.128	4.8	99.1	0.0676	1.0212
	R5-4-1	700	0.145	5.2	99.1	0.0725	1.0270
	R6-4-1	1953	0.193	2.0	99.1	0.00470	0.6858
Ishii et al. (2000)	C1P4	1886	0.193	0.9	90.7	0.0668	0.9945
	C2P2	942	0.193	1.0	53.5	0.1225	1.0235
	C2P4	942	0.193	1.0	90.7	0.5087	1.0887
	C3P4	1913	0.193	2.0	90.7	0.0295	0.9273
	C4P2	943	0.193	2.2	53.5	0.1588	1.0294
	C4P4	943	0.193	2.2	90.7	0.4129	1.0865
	C5P2	1413	0.193	3.6	53.5	0.0628	0.9738
	C6P2	951	0.193	3.9	53.5	0.1155	1.0063
	C6P4	951	0.193	3.9	90.7	0.3054	1.0731

increase in the value of the distribution parameter as the void profile develops. In view of the basic characteristic described above and various experimental data, Ishii proposed the following simple correlation as [Ishii, 1974]:

$$C_0 = \left(1.2 - 0.2\sqrt{\rho_g/\rho_f}\right) \left(1 - e^{A(\alpha)}\right), \quad (15)$$

where ρ_f and A are the liquid density and a coefficient, respectively, and Ishii recommended the coefficient to be -18. Since Eq.(15) was derived based on experimental data mainly taken in round tubes, the applicability of Eq.(15) to subcooled boiling flow in an internally heated annulus should be examined based on experimental data. As can be seen from Eq.(9), the distribution parameter can be determined provided that the profiles of void fraction and mixture volumetric flux are available. As explained in the section 4.1, some data on void fraction profile are available [Bartel et al., 2001; Ishii et al., 1999b; 2000]. However, since the profile of mixture volumetric flux is not available in the data base, the profile is approximated by Eq.(7) to determine the distribution parameter. In this calculation, n in Eq.(7) is assumed to be 7. Figure 3 shows an example of the sensitivity analysis of C_0 on n . Since 30 % change of n only causes ± 5 % deviation from the value of C_0 calculated by using $n=7$, a slight change of n may not affect C_0 significantly. Thus, n is approximated to be 7 in this study.

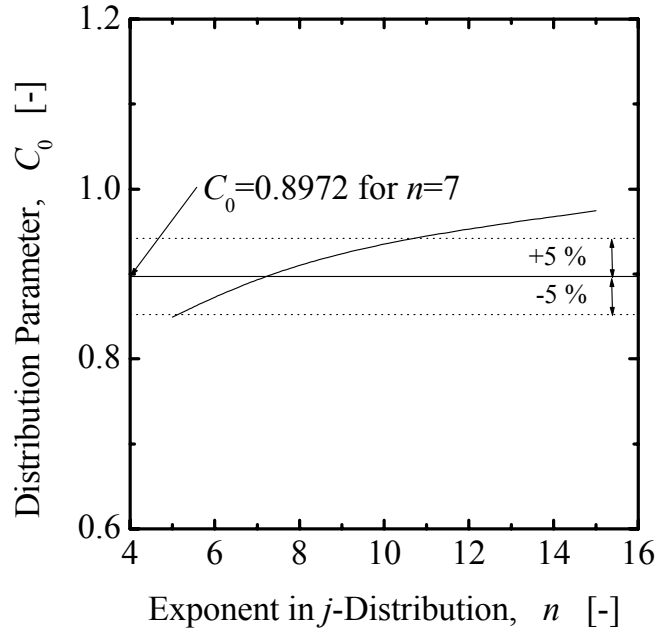


Fig.3. Dependence of distribution parameter on exponent in j -distribution.

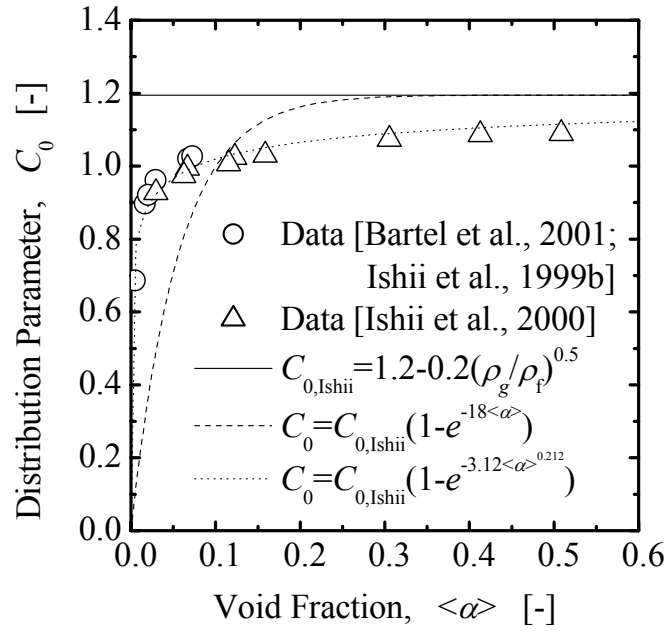


Fig.4. Comparison of newly developed constitutive equation for distribution parameter in an internally heated annulus with experimental data.

In Fig.4, the distribution parameters obtained based on the measured profile of the void fraction and the assumed profile of the mixture volumetric flux are plotted against the measured area-averaged void fraction. Solid and broken lines indicate the distribution parameters calculated by Ishii's equation for an adiabatic flow in a round tube, Eq.(16), and Ishii's equation for boiling flow in a round tube, namely Eq.(15) with $A=-18$.

$$C_0 = 1.2 - 0.2\sqrt{\rho_g/\rho_f}. \quad (16)$$

Unfortunately, both equations do not give good predictions of the distribution parameter for the internally heated annulus. The effect of the channel geometry on the distribution parameter may be attributed to the difference in the position where void peaking appears between channels. For an internally heated annulus, void fraction peak exists near the wall of the inner heater rod, whereas for a round tube, void fraction peak appears near the wall of the round tube. However, it is found from Fig.4 that the distribution parameter in the internally heated annulus appears to be still a function of the area-averaged void fraction and the asymptotic value of the distribution parameter may be given by Eq.(16). It should be noted here that the distribution parameters for an adiabatic bubbly flow in an annulus with the same dimensions as the internally heated annulus can approximately be represented by constitutive equation for distribution parameter of a bubbly flow in a round tube [Hibiki & Ishii, 2002; Hibiki et al., 2003]. This may be attributed to void fraction profile of the adiabatic flow observed in the annulus, which is similar to that in a round tube. Even in the annulus, two void peaks for the adiabatic flow appear in the vicinity of inner and outer tubes [Hibiki et al., 2003]. This phase distribution pattern is quite similar to that in the round tube, where two void peaks appear along the radius of the tube. Thus, a function similar to Eq.(15) may be recommended to develop a new constitutive equation for the distribution parameter in the internally heated annulus. The following explicit form of the coefficient, A , in Eq.(15) is plotted against the area-averaged void fraction in Fig.5.

$$A = \frac{1}{\langle \alpha \rangle} \ln \left(1 - \frac{C_0}{1.2 - 0.2\sqrt{\rho_g/\rho_f}} \right). \quad (17)$$

It is found that the coefficient is not constant and is a function of the area-averaged void fraction. The dependence of the coefficient on the area-averaged void fraction can be given by

$$A = -3.12\langle \alpha \rangle^{-0.788}. \quad (18)$$

Thus, the substituting Eq.(18) into Eq.(15) yields the constitutive equation for the distribution parameter of subcooled boiling flow in an internally heated annulus as:

$$C_0 = \left(1.2 - 0.2\sqrt{\rho_g/\rho_f} \right) \left(1 - e^{-3.12\langle \alpha \rangle^{0.212}} \right). \quad (19)$$

A dotted line in Fig.4 indicates the distribution parameter calculated by the newly developed equation,

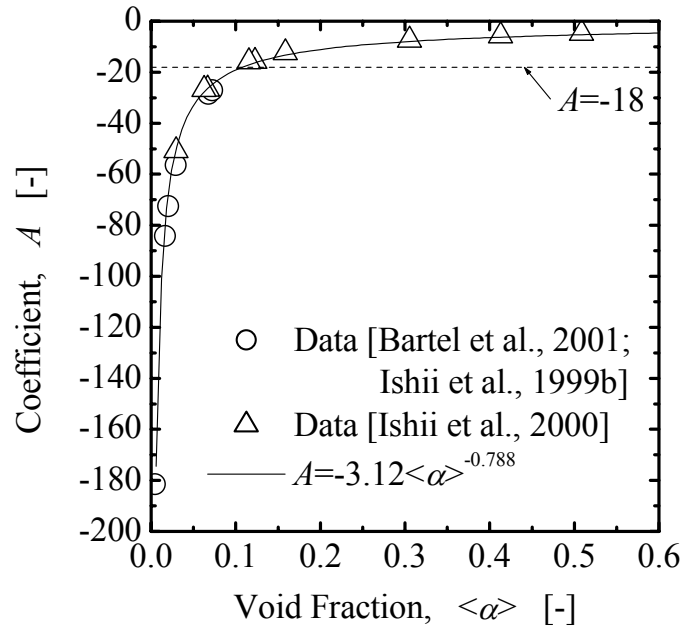


Fig.5. Dependence of coefficient, A , on area-averaged void fraction.

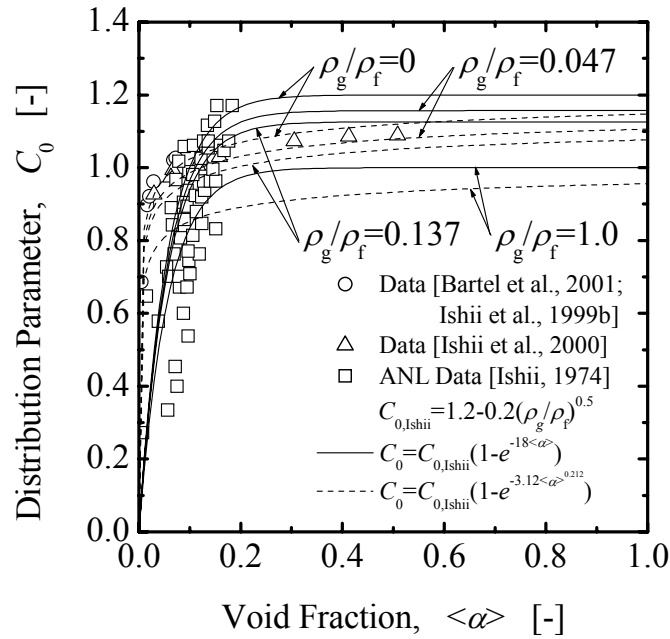


Fig.6. Comparison of newly developed constitutive equation for distribution parameter in an internally heated annulus with ANL data.

Eq.(19). As shown in the figure, the newly developed equation can represent the data tendency very well. Figure 6 compares the newly developed equation with the data used in the development of Ishii's equation for boiling flow in a round tube [Ishii, 1974]. Solid and broken lines indicate the predicted distribution parameters by Eq.(15) with $A=-18$ and Eq.(19), respectively. As expected, the newly developed correlation seems not to agree with the data taken in the round tubes satisfactorily, although the scatter of the data is relatively large. In the next section, the effect of the channel geometry on the distribution parameter will be discussed in detail.

4.3. Modification of Ishii's equation to estimate distribution parameter in annulus

In order to derive the distribution parameter of boiling flow for a round tube analytically, the profiles of mixture volumetric flux and void fraction are approximated by Eqs.(20) and (21), respectively.

$$j = \frac{n+2}{n} \langle j \rangle \left\{ 1 - \left(\frac{r}{R_p} \right)^n \right\}, \quad (20)$$

where r is the radial coordinate measured from the tube center, and the exponent, n , is approximated to be 7.

$$\begin{aligned} \alpha &= \alpha_{WP} \text{ for } R_p - x_{WP} \leq r \leq R_p \\ \alpha &= 0 \text{ for } 0 \leq r \leq R_p - x_{WP} \end{aligned}, \quad (21)$$

where R_p is the radius of the round tube, see Fig.7. From Eqs.(9), (20) and (21), one can obtain the distribution parameter for boiling flow in a round tube analytically as:

$$C_0 = \frac{n - \left(1 - \frac{x_{WP}}{R_p} \right)^2 \left\{ (n+2) - 2 \left(1 - \frac{x_{WP}}{R_p} \right)^n \right\}}{n \left\{ 1 - \left(1 - \frac{x_{WP}}{R_p} \right)^2 \right\}}. \quad (22)$$

As shown in Fig.8, the distribution parameters of boiling flow in internally heated annulus and round tube are plotted against the ratios of the bubble area, A_{WP} , to the channel area, A_C given by Eqs.(23) and (24), respectively.

$$\frac{A_{WP}}{A_C} = \frac{x_{WP}(2R_0 + x_{WP})}{R^2 - R_0^2}, \text{ for annulus,} \quad (23)$$

$$\frac{A_{WP}}{A_C} = 1 - \left(1 - \frac{x_{WP}}{R_p} \right)^2, \text{ for round tube,} \quad (24)$$

The figure indicates that the distribution parameter for the annulus is always higher than that for the round tube at a certain A_{WP}/A_C . Since the product of A_{WP}/A_C and α_{WP} is equal to $\langle \alpha \rangle$, A_{WP}/A_C may

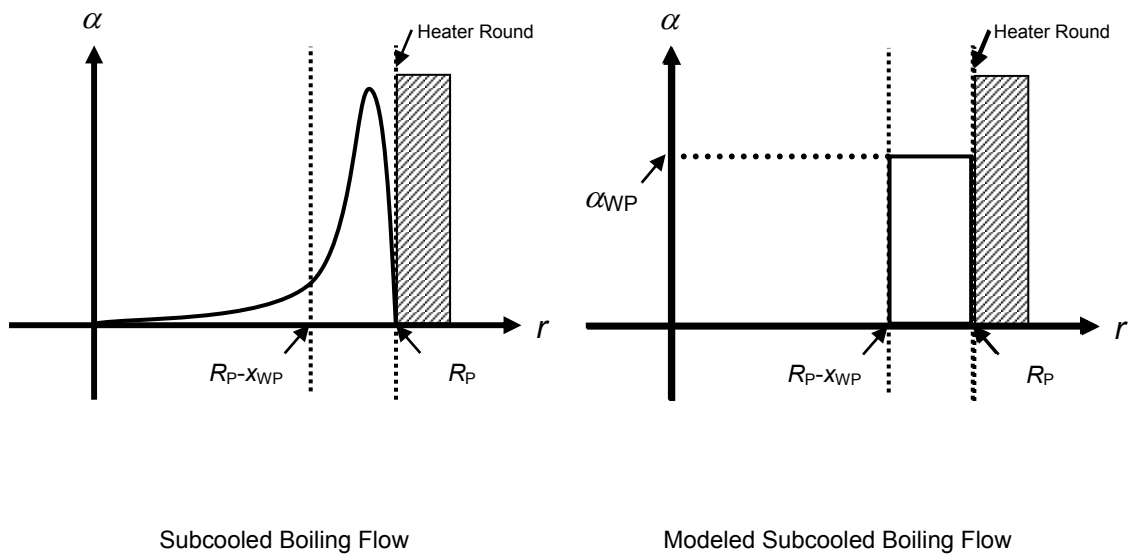


Fig.7. Schematic diagram of modeled subcooled boiling flow in bubble-layer thickness model for a round tube.

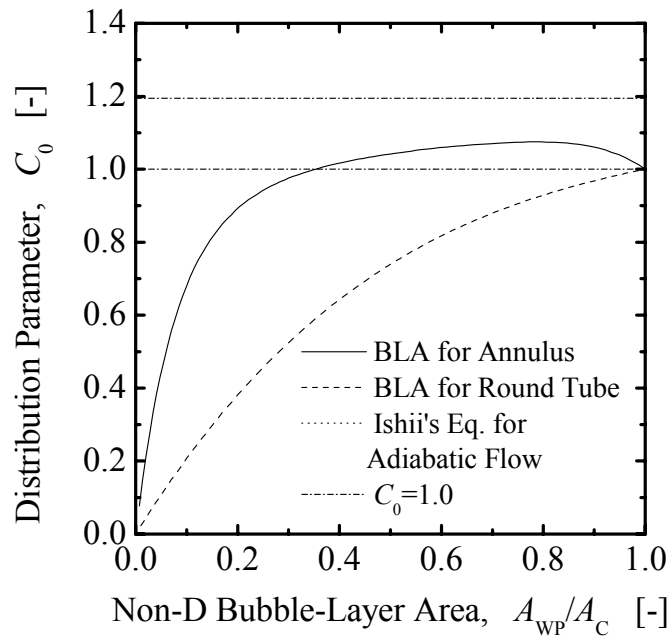


Fig.8. Dependence of distribution parameter on non-dimensional bubble-layer area.

correlate closely with $\langle\alpha\rangle$. If the relationship between $\langle\alpha\rangle$ and A_{WP}/A_C is identified in the annulus and the round tube, Ishii's equation for boiling flow in a round tube, Eq.(15), can be converted into a constitutive equation for the distribution parameter of boiling flow in an internally heated annulus. For the round tube, the relationship between $\langle\alpha\rangle$ and A_{WP}/A_C can be obtained from Eq.(15) with $A=-18$, and Eqs.(22) and (24). For the annulus, the relationship between $\langle\alpha\rangle$ and A_{WP}/A_C can be calculated from measured relationship between $\langle\alpha\rangle$ and C_0 , and Eqs.(10) and (23). Figure 9 shows the dependence of $\langle\alpha\rangle$ on A_{WP}/A_C . Open circles and a solid line represent the estimated relationships between $\langle\alpha\rangle$ and A_{WP}/A_C for the annulus and the round tube, respectively. For $A_{WP}/A_C \leq 0.3$, the dependence of $\langle\alpha\rangle$ on A_{WP}/A_C for the annulus agrees with that for the round tube fairly well. This indicates that α_{WP} as well as A_{WP}/A_C at a certain $\langle\alpha\rangle$ is the same between the annulus and the round tube for $A_{WP}/A_C \leq 0.3$. Therefore, for $A_{WP}/A_C \leq 0.3$, it can be considered that the difference in the dependence of C_0 on $\langle\alpha\rangle$ between the annulus and the round tube may mainly be attributed to the difference in the channel geometry. For $A_{WP}/A_C \leq 0.3$, the constitutive equation for the distribution parameter for boiling flow in the internally heated annulus can be obtained from Ishii's equation, Eq.(15), taking account of the channel geometry effect on the distribution parameter as:

$$C_0 = A \left(1.2 - 0.2 \sqrt{\rho_g / \rho_f} \right) \left(1 - e^{-18\langle\alpha\rangle} \right), \quad (25)$$

The modification factor, A , defined by the ratio of the distribution parameter for the annulus to that for the round tube is given as a function of the distribution parameter for the round tube, see Fig.10. A solid line indicates the modification factor obtained from Eqs.(10) and (22) analytically. However, the functional form is rather complicated, so the modification factor can be approximated as:

$$A = 5.30606 - 12.81133C_{0,Ishii} + 17.23067C_{0,Ishii}^2 - 11.86591C_{0,Ishii}^3 + 3.20513C_{0,Ishii}^4, \quad (26)$$

where $C_{0,Ishii}$ refers to the distribution parameter given by Eq.(15) with $A=-18$. In the figure, a broken line indicates the value calculated from Eq.(26). The approximated function, Eq.(26), can reproduce the exact values of the modification factor calculated from Eqs.(10) and (22) excellently. On the other hand, for $A_{WP}/A_C > 0.3$, the dependence of $\langle\alpha\rangle$ on A_{WP}/A_C for the annulus is significantly different from that for the round tube. However, as A_{WP}/A_C increases, the dependence of C_0 on $\langle\alpha\rangle$ becomes weaker. Thus, Eqs.(25) and (26) would practically be applicable even to the flow for $A_{WP}/A_C > 0.3$.

Figure 11 shows the comparison of calculated distribution parameters with experimental data taken in the internally heated annulus. Solid, broken, dotted, and chain lines indicate the distribution parameters calculated by Eq.(15), Eq.(19), Eq.(25) with exact modification factor, and Eq.(25) with approximated modification factor, Eq.(26), respectively. Since the exact modification factor is only available in the range of $0 \leq C_{0,Ishii} \leq 1.0$, namely $0 \leq \langle\alpha\rangle \leq 0.10$, the calculation of the distribution parameter is performed within the void fraction range. This limitation is attributed to assumed

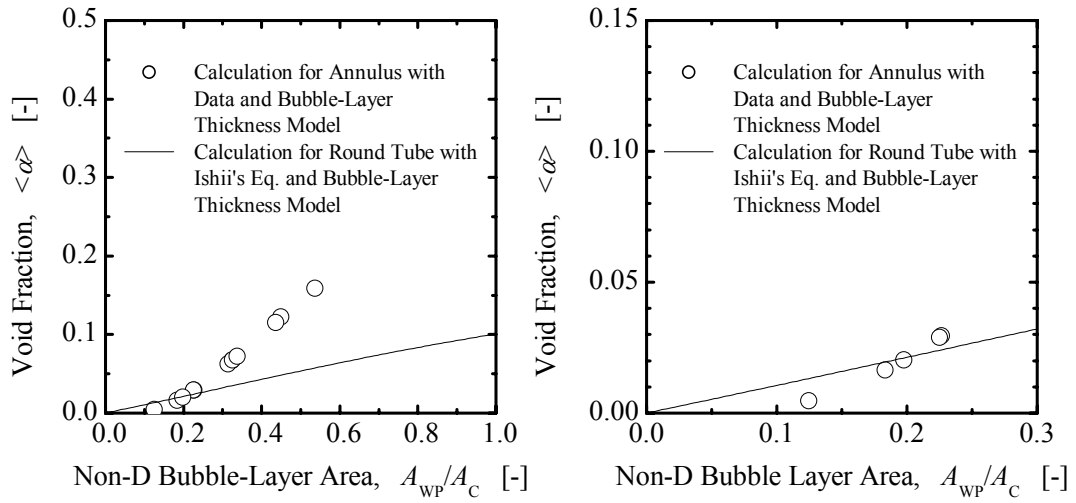


Fig.9. Dependence of area-averaged void fraction on non-dimensional bubble-layer area.

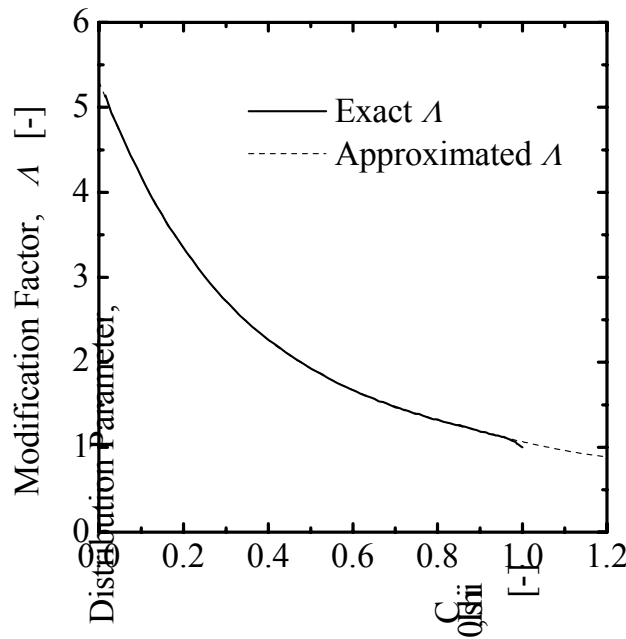


Fig.10. Comparison of exact modification factor with approximated one.

square void profile in the bubble-layer thickness model calculating the distribution parameter for the round tube. However, it would still be possible to calculate C_0 even in the range of $\langle \alpha \rangle \geq 0.10$ by Eq.(25) with extended use of Eq.(26). The distribution parameter calculated by Eq.(25) with Eq.(26) agrees with that calculated by Eq.(25) with the exact modification factor and with experimental data

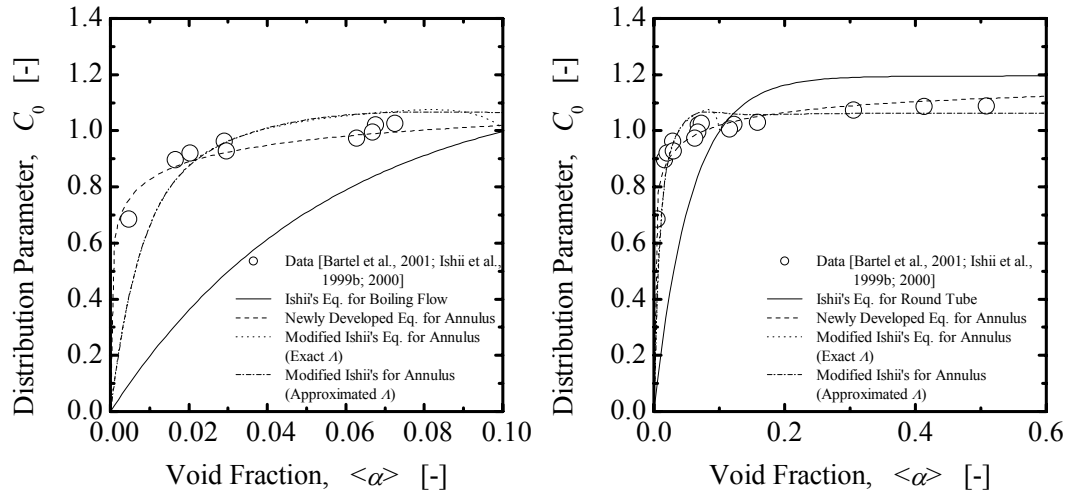


Fig.11. Comparison of distribution parameter for an internally heated annulus obtained by modifying Ishii's equation for a round tube with experimental data.

excellently. Thus, the distribution parameter obtained by modifying Ishii's equation for boiling flow in a round tube gives an excellent agreement with the experimental data taken in the internally heated annulus. This indicates that the difference in the dependence of C_0 on $\langle \alpha \rangle$ between the annulus and the round tube would mainly be attributed to the difference in the channel geometry. This extensive discussion on the effect of the channel geometry on the distribution parameter substantiates the validity of the physical mechanism how the distribution parameter develops with increase in the void fraction, which was proposed by Ishii [Ishii, 1974].

4.4. Flow parameter dependence of bubble-layer thickness

Figure 12 shows the dependence of flow parameters on the bubble-layer thickness calculated by using Eqs.(10) and (19). The figure at the upper left in Fig.12 shows the dependence of the distribution parameter on the bubble-layer thickness. As the bubble-layer thickness increases, the distribution parameter increases significantly in the region given by $0 \leq x_{WP}/(R-R_0) \leq 0.2$; beyond this region, the distribution parameter gradually increases to its maximum value ($C_{0,max}=1.07$); finally the distribution parameter reaches to 1.0 at $x_{WP}/(R-R_0)=1$. The figure at the upper right in Fig.12 shows the dependence of the area-averaged void fraction on the bubble-layer thickness. As the bubble-layer thickness increases, the area-averaged void fraction increases gradually in the region given by $0 \leq x_{WP}/(R-R_0) \leq 0.2$; beyond this region, the area-averaged void fraction steeply increases to its maximum value ($\langle \alpha \rangle = 0.241$); finally the area-averaged void fraction reaches to 0.0787 at

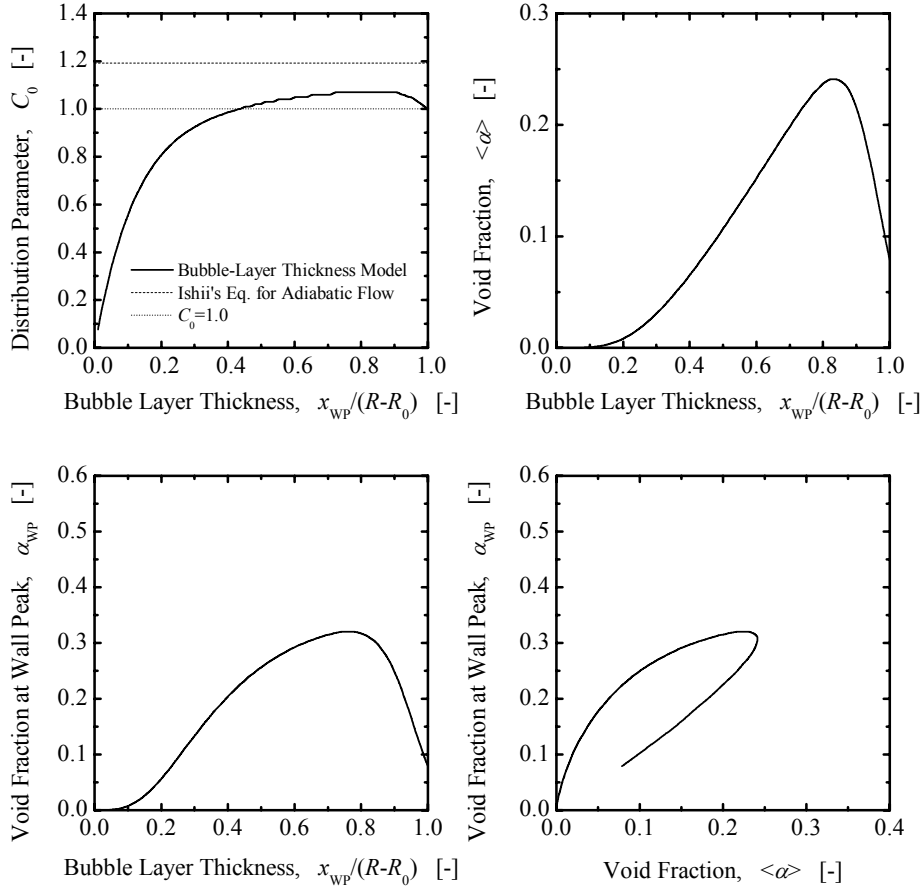


Fig.12. Flow parameter dependence of bubble-layer thickness calculated by bubble-layer thickness model.

$x_{wp}/(R-R_0)=1$. The figure at the lower left in Fig.12 shows the dependence of the void fraction at the wall peak on the bubble-layer thickness. As the bubble-layer thickness increases, the void fraction at the wall peak increases gradually in the region given by $0 \leq x_{wp}/(R-R_0) \leq 0.2$; beyond this region, the void fraction at the wall peak gradually increases to its maximum value ($\alpha_{wp}=0.320$); finally the distribution parameter reaches to 0.0787 at $x_{wp}/(R-R_0)=1$. The figure at the lower right in Fig.12 shows the dependence of the void fraction at the wall peak on the area-averaged void fraction. There are two values of the void fraction at the wall peak at a certain area-averaged void fraction in the region given by $0.0787 \leq \langle \alpha \rangle \leq 0.241$. Thus, in the region, a special attention should be paid in a numerical calculation determining the bubble-layer thickness. Figure 13 shows the dependence of flow parameters on the bubble-layer thickness calculated by using Eqs.(13) and (19). The dependence of flow parameters on the bubble-layer thickness is quite similar to that calculated by using the bubble-layer thickness model.

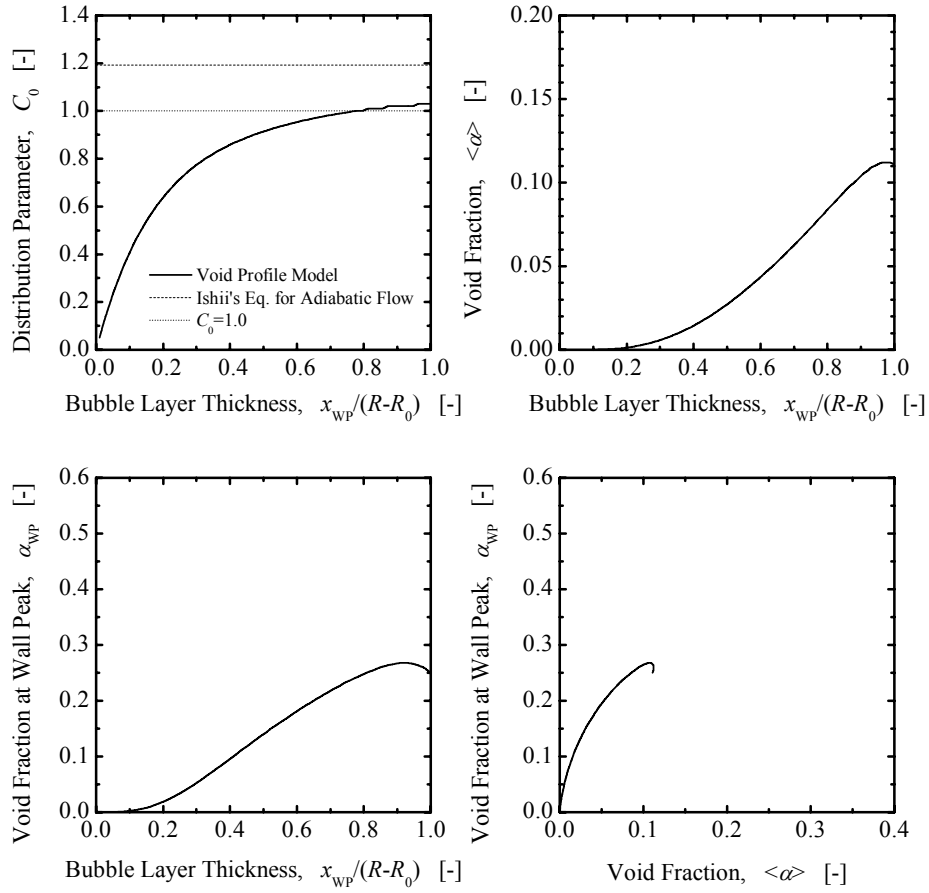


Fig.13. Flow parameter dependence of bubble-layer thickness calculated by void profile model.

4.5. Comparison of Bubble-Layer Model with Experimental Data

The bubble-layer thickness model, Eqs.(10) and (19), and void profile model, Eqs.(13) and (19), are compared with experimental data taken in an internally heated annulus [Bartel et al., 2001; Ishii et al., 1999b; 2000]. Typical results are shown in Fig.14. Open circles and solid lines indicate the measured void fraction profile, and its smoothed lines, respectively. Fine solid and broken lines are the void fraction profiles calculated by the bubble-layer thickness model and the void profile model, respectively. To emphasize the void fraction profile calculated by the bubble-layer thickness model, the void fraction profile is also shown in hatched area. As can be shown in Fig.14, the bubble-layer thickness model assuming the square void peak near a heated wall can approximate the measured void fraction profiles reasonably well. Thus, bubble-layer thickness model developed in this study would be sound and applicable to predict the bubble-layer thickness for subcooled boiling flow in an

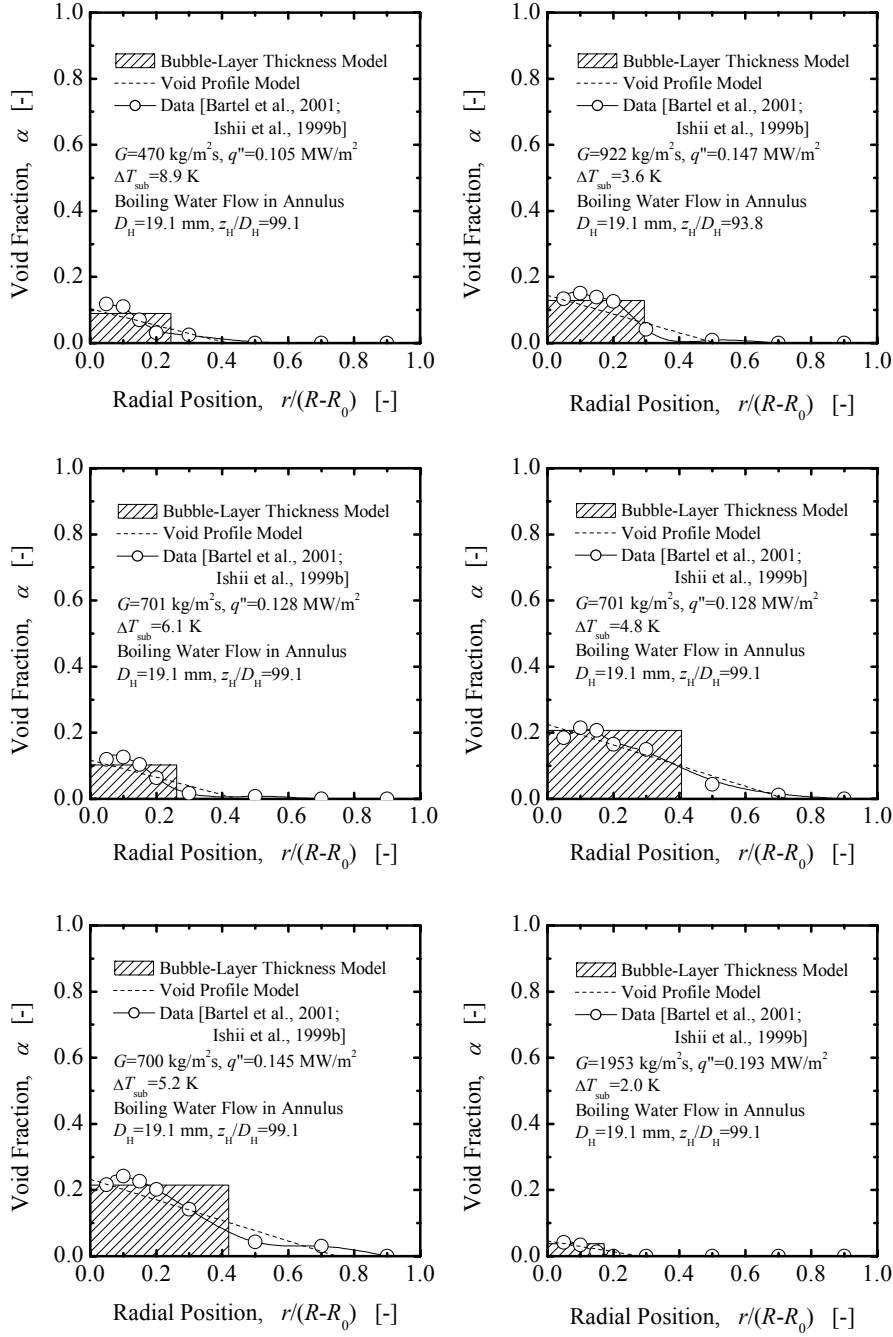


Fig.14. Comparison of void fraction profiles predicted by bubble-layer thickness and void profile models with experimental data.

internally heated annulus. Since the basic model utilized in this bubble-layer thickness model is considered to be sound, the bubble-layer thickness model in other channel geometries like a round tube and a rectangular duct can also be derived by taking account of the channel geometry and

distribution parameter. The void profile model assuming the right triangle void peak near a heated wall can represent the measured void fraction profiles better than the bubble-layer thickness model. Thus, the bubble-layer thickness and void profile models would be utilized for predicting the bubble-layer thickness to be used in the formulation of the one-dimensional interfacial area transport equation, and the void fraction profile, respectively. In a future study, the bubble-layer model and the constitutive equation for the distribution parameter developed in this study should be reevaluated based on extensive and rigorous data sets, and bubble-layer thickness model in other channel geometries should be developed based on the basic model proposed in this study.

5. CONCLUSIONS

In relation to the formulation of one-dimensional interfacial area transport equation in a subcooled boiling flow, the bubble-layer thickness model to predict the bubble-layer thickness was developed. Important results are as follows:

- (1) The one-dimensional interfacial area transport equation in a boiling flow was formulated by partitioning a flow region into two regions; boiling two-phase (bubble-layer) region and liquid single-phase region,
- (2) The bubble-layer thickness model assuming the square void peak in the bubble-layer region was developed to predict the bubble-layer thickness of boiling flow in an internally heated annulus,
- (3) The bubble-layer thickness model was compared with experimental data, and could successfully approximate the void fraction profile and predict the bubble-layer thickness,
- (4) The void profile model assuming the right triangle void peak in the bubble-layer region was developed to predict the void fraction profile of boiling flow in an internally heated annulus,
- (5) The void profile model was compared with experimental data, and could successfully approximate the void fraction profile,
- (6) In relation to the development of the bubble-layer thickness model, the constitutive equation for the distribution parameter in an internally heated annulus was developed,
- (7) It was shown that the constitutive equation for the distribution parameter for subcooled boiling flow in an internally heated annulus could be derived from Ishii's equation for boiling flow by considering the channel shape effect on the distribution parameter,
- (8) The void profiles predicted by the models were compared with experimental data taken for subcooled boiling water flows in an annulus. Excellent agreement was obtained between them.

The model developed in this study will eventually be used for the development of reliable constitutive relations, which reflect the true transfer mechanisms in subcooled boiling flows.

NOMENCLATURE

A	coefficient
A_B	area of the bubble-layer region
A_C	cross-sectional area
$A_i(V)$	average interfacial area
A_{WP}	ratio of the bubble area
a_i	interfacial area concentration
C_0	distribution parameter
$C_{0,Ishii}$	distribution parameter given by Ishii's equation for boiling flow in a round tube
D_{bc}	critical bubble size beyond which it is possible for bubbles to grow due to evaporation or for clusters of molecules to serve as nuclei for bubbles
D_e	sphere equivalent diameter
D_H	hydraulic equivalent diameter
D_{Sm}	Sauter mean diameter
dV	particle volume range
$d\bar{x}$	spatial range
$f(\bar{x}, V, t)$	particle density distribution function, which is assumed to be continuous and specifies the probable number density of fluid particles at a given time t , in the spatial range $d\bar{x}$ about a position \bar{x} , with particle volumes between V and $V+dV$
G	mass velocity
j	mixture volumetric flux
n	exponent
q''	heat flux
R	radius of outer round tube
R_j	rate of change of particle number due to coalescence or breakup
R_p	radius of the round tube
R_{ph}	rate of change of particle number due to phase change
R_0	radius of heated rod
r	radial coordinate measured from the heater rod surface or tube center
S_j	net rate of change in the particle density distribution due to the particle coalescence and breakup processes
S_{ph}	fluid particle source or sink rate due to the phase change

T_f	liquid temperature
T_{sat}	saturation temperature
t	time
V	particle volume
V_{max}	maximum particle volume
V_{min}	minimum particle volume
\bar{v}_g	gas-phase velocity
v_{gz}	z -component of gas-phase velocity
\bar{v}_p	particle velocity
x	radial coordinate measured from the center of the heated rod
\bar{x}	spatial position
z	axial coordinate
z_H	heated length

Greek symbols

α	void fraction
α_{WP}	void fraction at the assumed square void peak
Δi_{fg}	latent heat
ΔT_{sub}	liquid subcooling
Λ	modification factor
ρ_g	gas density
ρ_f	liquid density
σ	interfacial tension
ϕ_W	wall nucleation source
ψ	shape factor

Subscripts

max	maximum value
-----	---------------

Mathematical symbols

$\langle \rangle$	cross-sectional averaged quantity
$\langle \rangle_B$	quantity averaged over the bubble-layer region
$\langle \langle \rangle \rangle_B$	void fraction weighted quantity averaged the bubble-layer region

ACKNOWLEDGMENTS

The authors would like to express their sincere appreciation to Prof. J. M. Delhaye of Clemson University, USA for valuable discussions.

The research project was supported by the Tokyo Electric Power Company (TEPCO). The authors would like to express their sincere appreciation for the support and guidance from Dr. Mori of the TEPCO. Part of this work was supported by Grant-in-Aid for Scientific Research from the Ministry of Education, Science, Sport and Culture (No.:14580542).

REFERENCES

- M. D. Bartel, M. Ishii, T. Masukawa, Y. Mi, R. Situ, 2001, Interfacial area measurements in subcooled flow boiling, *Nuclear Engineering and Design*, **210**, pp.135-155.
- D. Ebert (Ed.), 1997, in: Proceedings of OECD/CSNI Workshop on Transient Thermal-hydraulic and Neutronic Codes Requirements, NUREG/CP-0159.
- M. Ishii, 1977, One-dimensional drift-flux model and constitutive equations for relative motion between phases in various two-phase flow regimes, ANL-77-47, USA.
- M. Ishii, 1996, Views on the future of thermal hydraulic modeling, Proceedings of the OECD/CSNI Workshop on Transient Thermal-Hydraulic and Neutronic Codes Requirements (NUREG/CP-0159), Annapolis, MD, USA, pp.751-759.
- M. Ishii, G. Kojasoy, 1993, Interfacial area transport equation and preliminary considerations for closure relations, PU/NE-93-6, School of Nuclear Engineering, Purdue University, USA.
- M. Ishii, Y. Mi, A. Assad, 1999a, Development and evaluation of one-group interfacial area transport equation, PU/NE-93-15, School of Nuclear Engineering, Purdue University, USA.
- M. Ishii, Y. Mi, M. D. Bartel, R. Situ, T. Masukawa, 1999b, Study of subcooled boiling in a vertical channel relevant to a boiling water reactor, PU/NE-93-30, School of Nuclear Engineering, Purdue University, USA.
- M. Ishii, Y. Mi, R. Situ, M. Mori, K. Tezuka, 2000, Experimental and theoretical investigation of subcooled boiling for numerical simulation Progress report 3, PU/NE-00-01, School of Nuclear Engineering, Purdue University, USA.
- T. Hibiki, M. Ishii, 2000a, One-group interfacial area transport of bubbly flows in vertical round tubes, *International Journal of Heat and Mass Transfer*, **43**, pp.2711-2726.
- T. Hibiki, M. Ishii, 2000b, Two-group interfacial area transport equations at bubbly-to-slug flow transition, *Nuclear Engineering and Design*, **202**, pp.39-76.
- T. Hibiki, T. Takamasa, M. Ishii, 2001, Interfacial area transport of bubbly flow in a small diameter pipe, *Journal of Nuclear Science and Technology*, **38**, pp.614-620.
- T. Hibiki, M. Ishii, 2002a, Distribution parameter and drift velocity of drift-flux model in bubbly flow, *International Journal of Heat and Mass Transfer*, **45**, pp.707-721
- T. Hibiki, M. Ishii, 2002b, Development of one-group interfacial area transport equation in bubbly flow systems, *International Journal of Heat and Mass Transfer*, **45**, pp.2351-2372.
- T. Hibiki, R. Situ, Y. Mi, M. Ishii, 2003, Local flow measurements of vertical upward bubbly flow in

- an annulus, *International Journal of Heat and Mass Transfer*, **46**, pp.1479-1496
- G. Kocamustafaogullari, M. Ishii, 1995, Foundation of the Interfacial Area Transport Equation and Its Closure relations, *International Journal of Heat and Mass Transfer*, **38**, pp.481-493.
- Shraiber, A. A., 1996, Comments on 'Foundation of the interfacial area transport equation and its closure relations', *International Journal of Heat and Mass Transfer*, **39**, pp.1117.
- J. Uhle, Q. Wu, M. Ishii, 1998, Dynamic flow regime modeling, in: Proceedings of 6th International Conference on Nuclear Engineering, San Diego, CA, USA, Paper No. ICONE-6509.
- Q. Wu, S. Kim, M. Ishii, S. G. Beus, 1998, One-group interfacial area transport in vertical bubbly flow, *International Journal of Heat and Mass Transfer*, **41**, pp.1103-1112.
- N. Zuber, J. A. Findlay, 1965, Average volumetric concentration in two-phase flow systems, *Journal of Heat Transfer*, **87**, pp.453-468.